Materials Science-Poland, 32(3), 2014, pp. 514-520
http://www.materialsscience.pwr.wroc.pl/
DOI: 10.2478/s13536-014-0225-x

VERSITA

Synthesis of porous ZnO nanostructures using bamboo fibers as templates

XIAOXUE LIAN*, YAN LI, DONGMIN AN, YUNLING ZOU, QIONG WANG, NAN ZHANG

College of Science, Civil Aviation University of China, Tianjin 300300, PR China

In this study, we fabricated ZnO nanostructures using bamboo fibers as templates. The starting material used was zinc acetate, and the nanostructures were synthesized by soaking and calcining the bamboo fibers. The fabricated nanostructures were characterized using X-ray powder diffraction (XRD) analysis, scanning electron microscopy (SEM), and ultraviolet-visible spectrophotometry. The results showed that the size of the ZnO nanoparticles was approximately 20 – 100 nm. When the ZnO nanoparticles were used as the catalyst in the photodegradation of methyl orange, the dye degraded by 95.98 % in 80 min. The response and recovery times of a gas sensor based on the ZnO nanoparticles were 25 and 24 s, respectively, during the detection of C_2H_5OH in a concentration of 10 ppm at 270 °C.

Keywords: *ZnO; bamboo fiber template; photocatalysis; gas sensitivity*

1. Introduction

Recently, ZnO has drawn significant attention owing to its large direct band gap (3.37 eV) and exciton binding energy (60 meV). It also possesses desirable catalytic, optical, electrical, and optoelectronic properties. Because of these properties ZnO is widely used as a photocatalyst [1] and in functional devices, such as solar cells [2], and sensors [3]. It is also used as a semiconductor [4]. ZnO structures with a number of morphologies have been fabricated. For example, Li et al. reported the fabrication of quantum-sized ZnO nanoparticles via the sol-gel method using sodium dodecyl sulfate as a surface modifier for toxic gases detection [5]. Hassan et al. fabricated ZnO nanorods by microwave-assisted chemical bath deposition, which were then used as hydrogen sensor at room temperature [6]. Lam et al. synthesized ZnO nanotubes for photocatalytic degradation of methylparaben via hydrothermal method using a ZnO powder and a 30 vol. % H_2O_2 aqueous solution [7]. Feng et al. prepared flower-like ZnO nanostructures via non-catalytic thermal evaporation, which had excellent optical properties [8]. Li et al. fabricated ZnO nanocombs via annealing, which had an effect on the morphologies and photoluminescence properties [9]. Using zinc nitrate hexahydrate as the starting material Kiomarsipour et al. synthesized scale- and spindle-like ZnO nanostructures exhibiting unique optical properties [10]. Therefore, it is essential to investigate new ZnO structures that can be used to extend the range of applications of ZnO.

Template-directed fabrication methods are used widely to prepare nanoparticles of various materials. In a typical process, the precursor material is assembled on the framework of the template, and then the porous nanomaterial is obtained once the template has been removed. The materials most commonly used as templates include polyethylene glycol (PEG) [11], copolymer gels [12], and polyvinylpyrrolidone (PVP) nanofibers [13]; these templates allow for the synthesis of hierarchical porous materials.

Biological materials with unique structures are plentiful in nature and are inexpensive and environmentally friendly. Some examples of biological entities with unique morphologies are bacteria [14] and butterfly wings [15]. Bamboo is used exten-

*E-mail: lianxiaoxues@163.com

sively to produce textiles due to its compact structure and smooth fibers. Therefore, bamboo fibers have been chosen as templates.

However, as far as anyone is aware, bamboo fibers have never been used as templates to form multilevel structures.

In this study, the synthesis of porous ZnO nanostructures using bamboo fibers as templates was investigated and the photocatalystic and gassensing properties of the thus synthesized nanoparticles were analysed.

2. Experimental

In order to remove hemicellulose, lignin, and other non-cellulose constituents from the surfaces of bamboo fibers, it was essential to pretreat the bamboo powder used as the starting material. First, 20 g of the bamboo powder (100 mesh) was placed in a beaker containing an aqueous solution of ammonium bicarbonate (NH_4HCO_3/H_2O = 20 g: 500 ml). The solution was then boiled for 5 – 7 min. After the solution was cooled, the powder was filtered from it. Next, the bamboo powder was rinsed with distilled water and placed in a beaker containing an acetic acid solution (4 %). The bamboo powder obtained after filtration was added to a solution of cetyltrimethylammonium bromide (CTAB) in ethanol (CTAB/ ethanol = 0.5 g: 200 ml) soaked in it for 24 h, filtered out, and dried in air.

The pretreated powder was added to a mixture of 0.2 mol/L of zinc acetate (150 mL) and 15 mL of ethanol and allowed to soak in it for 48 h. Subsequently, the powder was filtered out and dried in air. The bamboo powder was then calcined in a muffle furnace at 600 °C for 6 h, after which its weight stabilized.

The growth mechanism for synthesizing the hierarchically organized porous ZnO nanomaterial is shown in Fig. 1. First, the precursor was deposited on the cell walls of the pretreated bamboo fibers, then the precursor-loaded bamboo fibers were dried in air, resulting in secondary growth and the formation of a ZnO/bamboo composite. The porous nanostructures were obtained after the removal of the bamboo fibers through calcination in air.

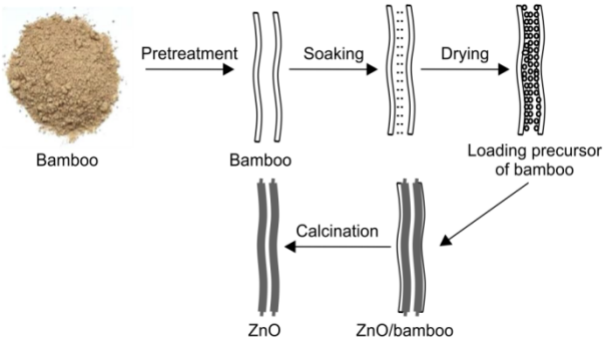

Fig. 1. Schematic illustration of the fabrication of hierarchically organized porous ZnO nanomaterial from bamboo tissue. A single fiber is used to illustrate the fabrication procedure.

The porous ZnO nanoparticles were examined using X-ray powder diffraction (XRD) analysis (DX-2000, Dandong Fangyuan); scanning electron microscopy (SEM) 1530 VP, and ultraviolet-visible spectrophotometer (WGZ-8, TianjinGangdong), a chemical gas sensing analysis system (CGS-8, Beijing Elite) and a self-assemblied photocatalytic device with a UV lamp (PLS-LAM 250) were also employed for this purpose.

The synthesized ZnO nanostructures were also used as the catalyst for the photocatalytic decomposition of methyl orange under UV irradiation for different time intervals. The methyl orange dye (20 mg) was dissolved in 1L of deionized water, and the fabricated ZnO powder (50 mg) was added in it. The suspension was first stirred for 0.5 h in darkness to reach the adsorption-desorption equilibrium of the methyl orange molecules on the surface of ZnO nanocatalyst and gain a good dispersion before irradiation, and then, the catalyst was placed under the UV lamp to irradiate for different time. The concentration of methyl orange solution was measured at regular time intervals during the irradiation and the solution taken out from the reactor was centrifuged to obtain a clear liquid. The change of methyl orange concentration was analyzed by a UV-Vis spectrophotometer (WGZ-8).The degradation rate of methyl orange was estimated using the following equation: degradation

rate (%) = $(A_0 - A)/A_0 \times 100$ %, where A_0 represents the initial absorbance of methyl orange and A denotes the absorbance at the time of measurement.

The sensitivity of the synthesized ZnO nanostructures was measured using chemical gas sensing system as reported by Liu et al. [16]. An n-type ZnO-based gas sensor was fabricated (Fig. 2). A certain amount of C_2H_5OH gas was injected into the testing container through a syringe, such that the concentration of the gas in the container was 10, 20, 50, or 100 ppm. The ZnO-based sensor was used to detect the gas at these concentrations [17–19]. The response of the ZnO-based sensor with respect to the reducing gas, C_2H_5OH, was defined as Ra/Rg, where Ra and Rg were the resistances of the ZnO-based sensor in air and in the target gas, respectively.

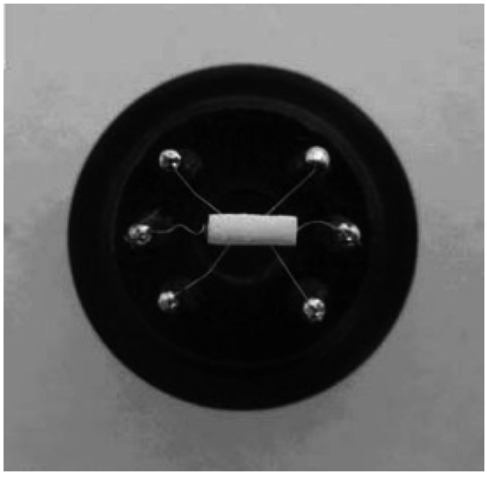

Fig. 2. A photograph of the ZnO-based gas sensor.

3. Results and discussion

The XRD pattern of the synthesized ZnO nanoparticles is shown in Fig. 3. All the diffraction peaks could be indexed to the hexagonal wurtzite phase of ZnO (JCPDS File No.: 36-1451). The high and sharp peaks are associated with the grain size of the ZnO crystallites. Crystallite size of the powders can be calculated through the Scherrer equation:

$$d_{Crys} = 0.89\lambda/(B\cos\theta)$$

where d_{Crys} is crystallite size, λ is the Cu $K_{\alpha 1}$ weighted average wavelength, B is the full width at half maximum for the diffraction peak under consideration, and θ is the diffraction angle. The average crystallite size calculated from the diffraction peaks of the (101), (100) and (002) crystal faces is 27 nm. No peaks attributable to any impurity were observed. This confirmed that the synthesized ZnO nanostructures were highly pure and crystalline.

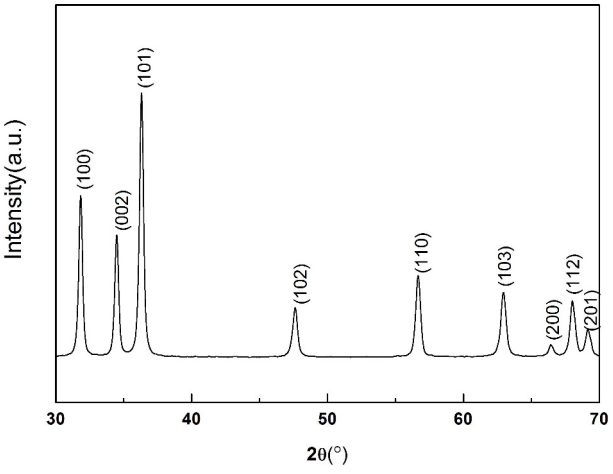

Fig. 3. XRD pattern of the synthesized nanoparticles.

To replicate both the macro- and microstructure of a bamboo tissue faithfully, it is necessary to generate very thin and continuous ZnO membranes on the cell walls [20]. In order to replicate the structure of bamboo tissue, it was adopted the soaking method for synthesis, which was not carried out in hydrothermal conditions because the size of the crystals obtained using the latter method is of the order of micrometers, which is different from that of the bamboo cells. Fig. 4a – 4c show the top-view, cross-sectional view, and side-view SEM images of the ZnO nanostructures, respectively; a SEM image of the wall structure is shown in Fig. 4d. As it can be seen from Fig. 4d, the pores formed from the bamboo template are nonuniform and 2 – 20 μm in size. The nanoparticles have a structure quite similar to that of bamboo fibers and replicate the morphologies of bamboo cells. Thus, this method of using bamboo fibers as templates can be a novel way to study bio-systems. The synthesized ZnO nanoparticles exhibit structural features, such as a

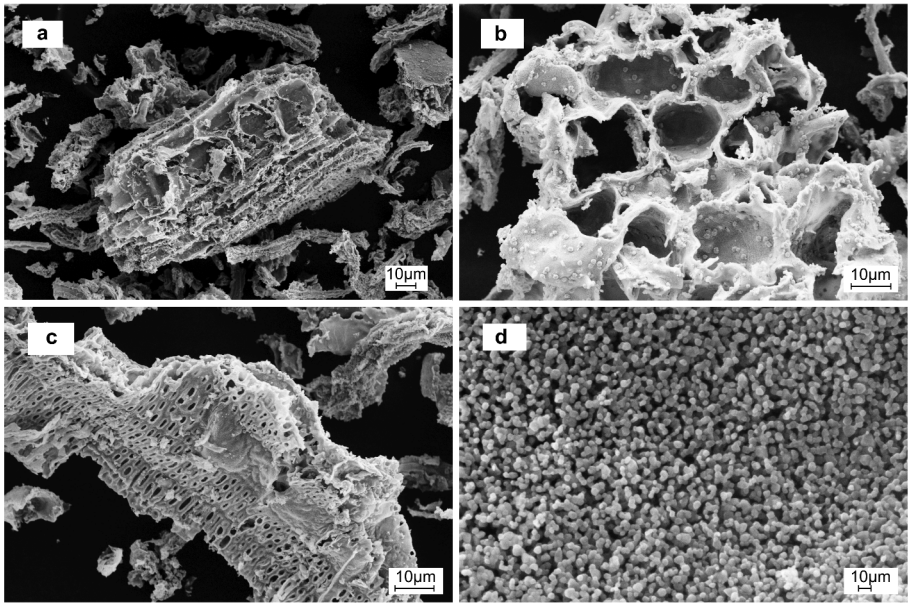

Fig. 4. (a – c). Top-view, cross-sectional view, and side-view SEM images of ZnO nanostructures, respectively. (d) SEM image of the wall structure of the ZnO nanostructures.

hierarchical arrangement (Fig. 4c). During the removal of the bamboo template through calcinations in air, the bamboo/ZnO composite emits certain amounts of CO_2 and H_2O, leading to the hierarchical holes observed in the walls of the porous ZnO nanomaterial. The ZnO nanoparticles were piled one on top of another, as it can be seen clearly from the SEM image in Fig. 4d. The image also shows that the diameters of the ZnO nanoparticles were approximately 20 – 100 nm, with most of the particles being 50 nm in size. Such ZnO nanostructures would be useful for photocatalysis and in sensors.

The photocatalytic activity of the synthesized nanoparticles was examined by using them as a catalyst in the degradation of methyl orange under UV irradiation. Fig. 5a shows the absorption spectra of the methyl orange solution (200 mL, 20 mg/L) in the presence of the synthesized ZnO nanoparticles (50 mg) under UV light irradiation for 10, 20, 30, 40, 50, 60, 70, and 80 min. The intensity of the highest absorption peak of methyl orange – analyzed by a UV-Vis spectrophotometer, which was located at a distance of 468 nm – decreased gradually with the increase in the exposure time, demonstrating that dye concentration decreased with the increase in exposure time. It could be confirmed from Fig. 5b that 95.98 % of the methyl orange was degraded after UV irradiation for 80 min and that most of it was degraded within 60 min. This was suggestive of the high activity of the synthesized ZnO nanoparticles as a photocatalyst. As it can be seen from Fig. 4, the bamboo fiber-like ZnO nanoparticles have multiple types of holes, which are very useful during photocatalysis and have a significant impact on the chemical and physical characteristics of ZnO as a photocatalyst. The methyl orange was degraded into the small molecules – that were either slightly toxic or non-toxic – as well as into CO_2 and H_2O [21].

The gas-sensing ability of the synthesized nanoparticles was investigated at different operating temperatures to determine the best conditions, under which the sensitivity was the highest. Fig. 6a shows the relationship between operating temperature and the sensitivity of the sensor with respect to 10 ppm of C_2H_5OH (g). The response of the ZnO-based sensor increased and reached its highest value at 270 °C; then it decreased with a further increase in the temperature. This phenomenon can be explained on the basis of the mechanics and kinetics of gas adsorption and desorption over the surfaces of ZnO nanoparticles [22].

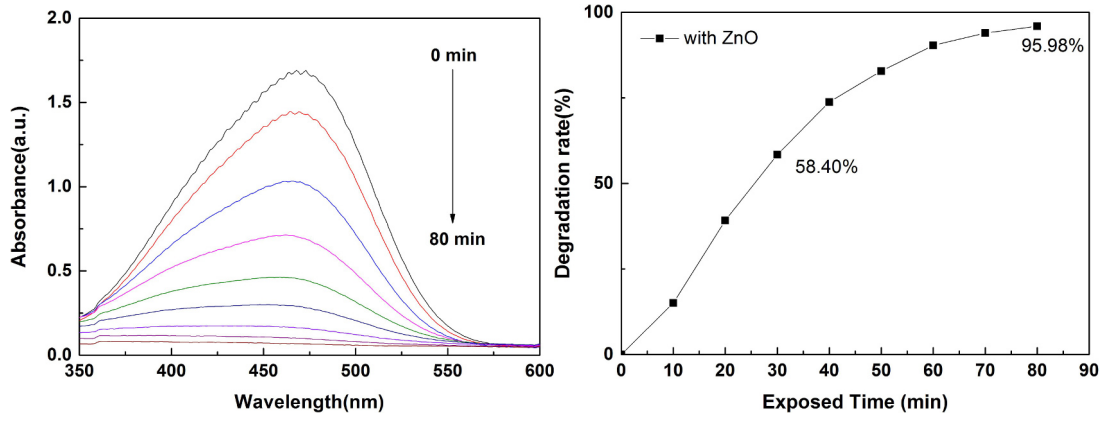

(a) (b)

Fig. 5. (a) Ultraviolet-visible absorbance spectra of the methyl orange solution irradiated with light in the presence of the synthesized ZnO nanoparticles and (b) the degradation rate (%) as a function of the irradiation time.

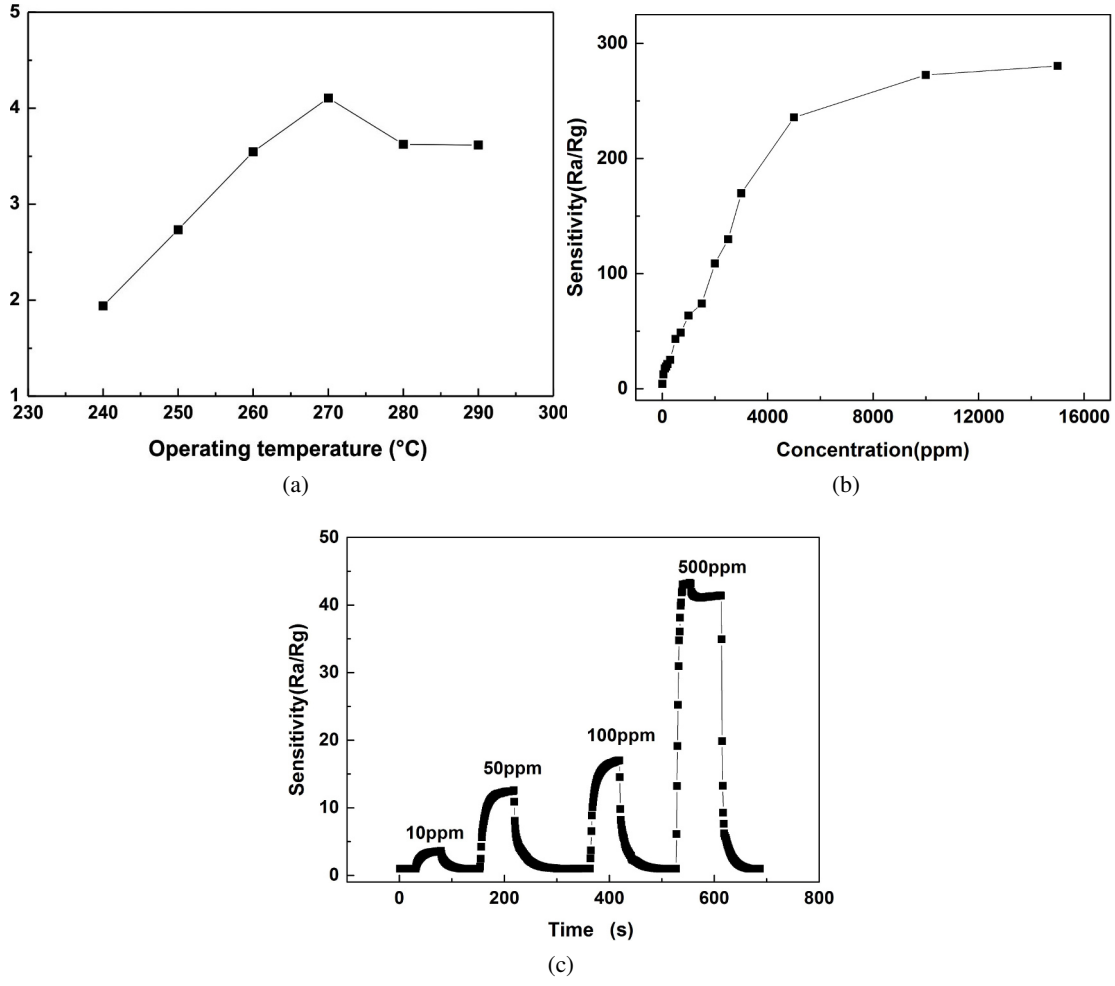

(a) (b) (c)

Fig. 6. (a) Response of the ZnO-based sensor to 10 ppm C_2H_5OH as a function of the operating temperature, (b) dependence of the response on the C_2H_5OH concentration, and (c) response and recovery curves of the sensor with respect to C_2H_5OH in the concentrations of 10 – 500 ppm at 270 °C.

Fig. 6b shows the responses of the ZnO-based sensor to different concentrations of C_2H_5OH (10 – 15000 ppm) at 270 °C. It can be seen that, even at the lowest concentration (i.e. at 10 ppm), the sensitivity is greater than 4. Further, the sensitivity increased rapidly for an increase in the C_2H_5OH concentration at the levels lower than 5000 ppm. From Fig. 6b it can be seen that there is a linear relationship between the sensitivity and the gas concentration (at concentration lower than 5000 ppm).

Table 1. Response times and recovery times of ZnO sensors to 10 – 500 ppm C_2H_5OH at 270 °C.

C_2H_5OH Conc. (ppm)	Response time (s)	Recovery time (s)
10	25	24
50	35	42
100	27	39
500	10	29

Fig. 6c shows the response and recovery curves of the ZnO-based sensors with respect to 10 – 500 ppm C_2H_5OH at an operating temperature of 270 °C. It is known that the response and recovery characteristics of ethanol sensors are direct indicators of their performance. To determine the response-recovery behavior of the sensor, it was directly exposed to 10, 50, 100, and 500 ppm C_2H_5OH at 270 °C. As can be seen from Fig. 6c, the sensor exhibited fast response and recovery during the sensing of C_2H_5OH. The response and recovery times of the sensor, calculated from Fig. 6c, are listed in Table 1. The ZnO-based sensor exhibited response times of approximately 25, 33, 27, and 10 s for C_2H_5OH concentrations of 10, 50, 100, and 500 ppm, respectively. Further, the recovery times of the sensor were approximately 24, 42, 39, and 29 s, respectively. The excellent response and recovery performance of the sensor was owing to the structure of the synthesized ZnO nanoparticles provided that their bamboo fiber-like structure nanoparticles did not undergo agglomeration. Therefore, the active surface area of the sensing material remained high, resulting in a high electron transfer rate. The unique structure of the sensing material also accelerated the transfer of the ethanol molecules to and from the interaction sites [23], resulting in the high sensitivity with respect to the detection of ethanol gas.

4. Conclusions

Porous ZnO nanostructures were synthesized using bamboo fibers as templates. The nanostructures were highly pure and crystalline, and their structure was similar to that of the bamboo fibers. The nanostructures were used as a photocatalyst in the photodegradation of methyl orange, which could be degraded by 95.98 % within 80 min upon UV irradiation. In addition, the nanostructures were employed as the sensing material in a sensor for C_2H_5OH. The temperature corresponding to the highest sensitivity was at 270 °C, and the sensitivity was found to increase with an increase in the C_2H_5OH concentration. The synthesized ZnO nanostructures exhibited response-recovery performance owing to their unique bamboo fiber-like structure. These results indicate that using bamboo fibers as templates is a promising approach for fabricating high-performance materials with unique structures inexpensively.

Acknowledgements

This work has been jointly supported by the Fundamental Research Funds for the Central Universities (Grant No. 3122013p001) and the Science and Technology Innovation Guide Funds of Civil Aviation Administration of China (2014). We also wish to thank the Applied Basic and Cutting-edge Research Programs of Science and Technology Foundation of Tianjin for support (Grant No. 13JCQNJC07100).

References

[1] Faisal M., Khan S.B., Jamal A., Abdullah M.M., *Appl. Surf. Sci.*, 258 (2012), 7515.
[2] Guerin V.M., Rathousky J., Pauporte T., *Sol. Energ. Mat. Sol. C.*, 102 (2012), 8.
[3] Phan D.T., Chung G.S., *Sensor. Actuat. B-Chem.*, 161 (2012), 341.
[4] Ates T., Tatar C., Yakuphanoglu F., *Sensor. Actuat. A-Phys.*, 190 (2012), 153.
[5] Li D.Q., Hu J.W., Fan F.Y., Bai S.L., Luo R.X., Chen A.F., Liu C.C., *J. Alloy. Compd.*, 539 (2012), 205.
[6] Hassan J.J., Mahdi M.A., Chin C.W., Abu-Hassan H., Hassan Z., *Sensor. Actuat. B-Chem.*, 176 (2012), 360.

[7] LAM S.M., SIN J.C., ABDULLAH A.Z., MOHAMED A.R., *Mater. Lett.*, 93 (2012), 423.
[8] FENG L.B., LIU A.H., LIU M., MA Y.Y., WEI J., MAN B.Y., *J. Alloy. Compd.*, 492 (2010), 427.
[9] LI Q., CHEN Y.Q., ZHANG X.H., SU Y., JIA C., *J. Phys. Chem. Solids*, 70 (2009), 1482.
[10] KIOMARSIPOUR N., RAZAVI R.S., *Ceram. Int.*, 39 (2012), 813.
[11] LIU Z.F., JIN Z. G., LI W., QIU J.J., *Mater. Lett.*, 59 (2005), 3620.
[12] JIU J.T., KURUMADA K., TANIGAKI M., *Mater. Chem. Phys.*, 81 (2003), 93.
[13] FANG X., LI S., WANG X., FANG F., CHU X., WEI Z., LI J., CHEN X., WANG F., *Appl. Surf. Sci.*, 263 (2012), 14.
[14] ZHANG H., XU C., SHENG P., CHEN Y., YU L., LI Q., *Sensor. Actuat. B-Chem.*, 181 (2013), 99.
[15] ZHANG W., ZHANG D., FAN T., DING J., GUO Q., OGAWA H., *Micropor. Mesopor. Mat.*, 92 (2006), 227.
[16] LIU L., GUO C., LI S., WANG L., DONG Q., LI W., *Sensor. Actuat. B-Chem.*, 150 (2010), 806.
[17] WEI S.H., WANG S.M., ZHANG Y., ZHOU M.H., *Sensor. Actuat. B-Chem.*, 192 (2014), 480.
[18] BAGHERI M., HAMEDANI N.F., MAHJOUB A.R., KHODADADI A.A., MORTAZAVI Y., *Sensor. Actuat. B-Chem.*, 191 (2014), 283.
[19] LEE Y.M., HUANG C.M., CHEN H.W., YANG H.W., *Sensor. Actuat. A-Phys.*, 189 (2013), 307.
[20] DONG A.G., WANG Y., TANG Y., REN N., ZHANG Y., YUE Y., GAO Z., *Adv. Mater.*, 14 (2002), 926.
[21] LIN D.D., WU H., ZHANG R., ZHANG W., PAN W., *J. Am. Ceram. Soc.*, 93 (2010), 3384.
[22] YAMAZOE N., FUCHIGAMI J., KISHIKAWA M., SEIYAMA T., *Surf. Sci.*, 86 (1979), 335.
[23] LI Z., ZHANG H., ZHENG W., WANG W., HUANG H., WANG C., MACDIARMID A.G., WEI Y., *J. Am. Chem. Soc.*, 130 (2008), 5036.

Received 2014-03-28
Accepted 2014-06-23